Gas-Phase Chemistry of Curium: Reactions of Cm^+ and CmO^+ with Alkenes, Acetonitrile, and Hexafluoropropene

John K. Gibson* and Richard G. Haire

Chemical and Analytical Sciences Division, Oak Ridge National Laboratory, Oak Ridge, Tennessee 37831-6375

Received: September 3, 1998; In Final Form: October 26, 1998

The metal ions, Cm^+, U^+, and Tb^+, and their oxides, MO^+, were reacted in the gas phase with alkenes, acetonitrile, and hexafluoropropene. Product compositions and abundances provide a survey of essential aspects of the gas-phase chemistry of the curium cation, now the heaviest element for which such systematic studies have been carried out (U and Tb were included to provide comparisons). Of particular interest is the difference in behavior between the 4f lanthanide and 5f actinide series and variations in chemistry across the actinide series. The primary emphasis was on reactions with alkenes, particularly dehydrogenation, as indicative of the ability of a M^+ to activate C−H bonds (the extent of C−C activation was generally in parallel with that of C−H activation). With acetonitrile and all of the alkenes (except ethene), the three M^+ ions induced dehydrogenation. Variations were evident for the different reactant substrates, but the overall qualitative ordering of dehydrogenation efficiency was $U^+ > Tb^+ > Cm^+$. This order is consistent with the variation in electronic promotion energies (PE) required to provide two spin-unpaired, non-f valence electrons at the M^+, i.e., a $[Rg]f^{n-2}d^1s^1$ configuration ("Rg" = Xe for the lanthanides and Rn for the actinides), to enable its insertion into a C−H bond. The reduced reactivity of Cm^+ relative to U^+ and Tb^+ suggests that the closed-shell $7s^2$ electrons of ground Cm^+ (^8S $[Rn]5f^7s^2$) are ineffective in enabling C−H activation and that promotion to the ^{10}D $[Rn]5f^76d^17s^1$ configuration is prerequisite. The PE[Cm^+] (48 kJ mol^{-1}) is only slightly greater than PE[Tb^+] (39 kJ mol^{-1}) and the significantly greater reactivity of Tb^+ vs Cm^+ may reflect that the transition to the prepared "divalent" state (d^1s^1) is parity forbidden for Cm^+. The three MO^+ were substantially less reactive than the naked M^+ but were comparably reactive to one another, consistent with a multicentered activation process, which is less efficient than direct cleavage of a C−H bond by M^+ insertion. With hexafluoropropene, the primary reaction channel was F abstraction and the discrepant reactivities reflected the propensity for U to oxidize to higher valence states compared to Cm or Tb. The terminal MF_n^+ were $Cm^{III}F_2^+$, $Tb^{III}F_2^+$, and $U^{IV}F_4^+$, and among the MO^+, only UO^+ induced F abstraction, producing UOF_n^+ with $n = 1-3$.

Introduction

Gas-phase reactions between naked and ligated metal ions have developed into an effective tool for examining fundamental aspects of organometallic chemistry and reaction mechanisms under elementary conditions absent secondary effects encountered in the condensed phase. Most gas-phase investigations have focused on the prevalent and technologically important first-row transition elements, although the heavier d-block and inner f-block transition elements are now receiving increased attention.[1,2]

The diverse gas-phase chemistry of the lanthanide (Ln) elements is of particular interest in view of their similar chemistries in the condensed phase. Several studies of reactions of Ln^+ with hydrocarbons have been carried out,[3−5] and it has been established[4,5] that large variations in dehydrogenation and cracking efficiencies correlate with the energies required to excite the ground-state Ln^+ to an electronic configuration with two non-4f valence electrons. A $4f^{n-2}5d^16s^1$ configuration is evidently prerequisite for insertion of the Ln^+ into a C−H bond to produce the C−Ln^+−H intermediate, which precedes β-H abstraction and H_2 elimination. Cornehl, et al. examined reactions of LnO^+ with butadiene,[6] discovering a striking effect of oxoligation on the relative reactivities of the lanthanide ions, which was attributed to a noninsertion mechanism involving an electrostatically bonded, multicentered intermediate.

In contrast to the 4f Ln elements, the 5f electrons of the light actinide (An) elements can participate in covalent bonding, as a result of their greater spatial extension and energetic proximity to the 6d/7s valence electron levels. Extension of gas-phase reaction studies to An^+ and AnO^+ has the potential to illuminate distinctions between the behavior of the Ln and An elements and specifically the role of the 5f electrons in organometallic bonding and reaction mechanistics. Early studies of reactions of U^+ with CD_4, D_2, and N_2[7] were carried out by Armentrout et al., and recent investigations with Th^+, ThO^+, U^+, and UO^+ have been reported.[8−13] Both Th^+ and U^+ have ground electronic configurations with two non-5f electrons and accordingly exhibit high reaction efficiencies that do not illuminate explicitly the role of their 5f electrons. In contrast, the ground states of some heavier An^+ have only one non-5f valence electron (e.g., $[Rn]5f^{n-1}7s^1$). To extend gas-phase ion chemistry studies to transuranium (TRU) actinide ions, the technique of laser ablation with prompt reaction and detection (LAPRD) was developed in our laboratory. Relative reaction efficiencies determined for Np^+, Pu^+,[14] and Am^+,[15] $Np^+ > Pu^+ > Am^+$, established that promotion to an electronic configuration comprising two non-5f valence electrons (i.e., $[Rn]5f^{n-2}6d^17s^1$) is essential for effective C−H activation, presumably via a covalently bonded

* Corresponding author. E-mail: gibsonjk@ornl.gov.

10.1021/jp9836067 CCC: $15.00
Published on Web 12/08/1998

C−An$^+$−H intermediate. As with the Ln$^+$, oxoligation has been found to have a profound effect on An$^+$ reaction efficiencies.[11−14] All of the AnO$^+$ exhibit lower dehydrogenation efficiencies than the naked An$^+$, consistent with a relatively inefficient reaction mechanism involving a multicentered intermediate. An intriguing observation was the greater reactivity of UO$^+$ compared with NdO$^+$, an effect that might reflect participation of the 5f electrons at the metal center of UO$^+$.[13] Both NpO$^+$ and PuO$^+$ were found to be appreciably less reactive than UO$^+$,[14] perhaps indicating a transition from chemically active 5f electrons at the metal center of UO$^+$ to inert (localized) 5f electrons in TRU AnO$^+$.

Whereas the $5f^{n-1}7s^1 \rightarrow 5f^{n-2}6d^17s^1$ promotion energies increase from zero for Np$^+$ ($5f^46d^17s^1$ ground state) to 104 kJ mol^{-1} for Pu$^+$ and then to 245 kJ mol^{-1} for Am$^+$, the value decreases to 48 kJ mol^{-1} for Cm$^+$;[16] accordingly, Cm$^+$ represents a central member of the series of An$^+$, which should be quite reactive. In contrast to AmO$^+$, CmO$^+$ is a rather stable molecular ion and can be produced in sufficient quantities to assess its reactivity in comparison with lighter AnO$^+$. The primary goal of the present study was to extend the understanding of hydrocarbon dehydrogenation efficiencies for An$^+$ and AnO$^+$ to the next member of the actinide series, Cm. Laser-ablated Cm$^+$ and CmO$^+$ were reacted with a variety of alkene substrates, and the reaction efficiencies were compared directly with those for U$^+$, UO$^+$, Tb$^+$, and TbO$^+$. Uranium was included as a representative reactive light actinide that exhibits 5f bonding under certain conditions; Tb$^+$ was selected due to the similarity of its $f^{n-1}s^1 \rightarrow f^{n-2}d^1s^1$ promotion energy (39 kJ mol^{-1} Tb$^+$[17]) to that for Cm$^+$ (48 kJ mol^{-1} [16]).

Gas-phase reactions of transition metal ions with alkyl nitriles have received attention as the C≡N: functionality offers an effective but relatively inert cation coordination site.[18,19] Dehydrogenation and other reactions involving the alkyl group have been demonstrated with unusual selectivity effected by what Schwarz and co-workers have termed "remote functionalization".[16] Previously, selected Ln$^+$ and An$^+$ were reacted with several nitriles in our laboratory,[20] resulting in both adduct formation, presumably by coordination to the N: moiety, and alkyl dehydrogenation. Alkyl dehydrogenation was particularly noteworthy in view of the inert behavior of Ln$^+$ and An$^+$ toward unfunctionalized alkanes. Dehydrogenation of acetonitrile resulted in complex ions which were presumed to be novel carbene species, M$^+$=(CH)−C≡N. Acetonitrile was reacted with Cm$^+$ and CmO$^+$ in the present study.

The LAPRD technique has been employed previously to study reactions of Ln$^+$,[21−23] An$^+$, and AnO$^+$ [24] with fluorocarbons, C_nF_m. The primary reaction pathway was F abstraction to produce MF_n^+ and MOF_n^+, with the highest values of n for a given Ln or An reflecting the propensity to form higher oxidation states. In contrast to the lanthanides, which exhibit predominantly trivalent chemistry in the condensed phase, the light actinides may exhibit a variety of oxidation states (e.g., III−VII for Np). In the present study, Cm$^+$ was reacted with C_3F_6 and the oxidation (F abstraction) behavior of Cm$^+$ was compared with that of U$^+$.

Experimental Section

The LAPRD method and its application to TRU actinide ions has been described elsewhere,[5,11,14,15,20,23,24] and only a summary of essential features of the experiment is included here. The output of a XeCl (308 nm) excimer laser was attenuated and focused at normal incidence onto the ablation target to a spot size of ∼0.5 mm^2 to produce a nominal irradiance in the range of 10^7-10^8 W cm^{-2}. The ablated material propagated ∼3 cm through a reactant gas, which was injected into the ablation plume trajectory either through a continuous leak valve or a pulsed solenoid valve. The local pressure was indeterminate, but formation of bisnitrile adduct products under comparable conditions[20] indicated that most ablated ions underwent multiple collisions with reactant molecules. After traveling ∼3 cm into the reflectron time-of-flight mass spectrometer (RTOF-MS) ion source, the unreacted and product positive ions from a ∼6 mm^2 cylindrical cross section of the expanding ablation plume were orthogonally injected into the RTOF-MS. The time delay, t_d, between the laser pulse and injection into the RTOF-MS was varied to obtain near optimal detection of product ions; although absolute ion intensities varied substantially with t_d, the comparative reactivities of the M$^+$ and MO$^+$ were essentially invariant with t_d. The employed t_d varied from 35 to 60 μs, with the longer values used predominantly for the pulsed valve experiments. The sampled ablated ions had approximate velocities of $v_I \approx \{3\text{ cm}/t_d\}$ (≈1 km s^{-1} for $t_d = 35$ μs and 0.5 km s^{-1} for $t_d = 60$ μs). All of the reactions involved hyperthermal ions, and the collisional energies (KE_{CM}) can be estimated from the ion kinetic energy, $KE_I = 1/2\{M_I\}\{v_I\}^2$ (M_I = ion mass), by assuming a quasistationary target molecule, R, of mass M_R: $KE_{CM} \approx KE_I\{M_R/(M_I + M_R)\}$. Typical values of KE_{CM} ranged from ∼5 kJ mol^{-1} (for Tb$^+$ + C_3H_6 sampled at $t_d = 60$ μs) to ∼30 kJ mol^{-1} (for Cm$^+$ + C_6H_6 sampled at $t_d = 35$ μs). For ^{248}Cm$^+$ and ^{238}U$^+$, the KE_{CM} values were nearly identical for a given reaction. The fact that the probed reactions apparently involved ablated ions in or near their ground electronic states has been discussed previously[5] and is probably attributable to the sampling of relatively slow ablated ions, an apparent advantage of orthogonal, time-delayed ion sampling.

Given the limited availability of ^{248}Cm, experiments with this isotope were especially challenging, and only one Cm-containing ablation target was studied. The Cm target was prepared by the technique described previously[14] where powders of the constituent metal oxides were blended with an excess of copper powder and then pressed into a durable pellet at room temperature. Whereas the targets comprising Np, Pu, and Am had been prepared with a 3 mm diameter pellet press, the Cm target was fabricated using a 1.6 mm diameter die, given the smaller quantity of Cm. The pellet constituents were 0.783 mg of Cm_7O_{12}, 0.605 mg of UO_2, 0.592 mg of Tb_4O_7, and 12.700 mg of Cu^o. This gave a composition (metals basis) of 1.4 atom % Cm, 1.1 atom % U, 1.5 atom % Tb, and 96 atom % Cu. All components except the Cm_7O_{12} were commercial products of ≥99.9% chemical purity. The Cm_7O_{12} was of comparable chemical purity, and the Cm was ∼97% ^{248}Cm and ∼3% ^{246}Cm; isotopically unspecified "Cm" in the text refers to ^{248}Cm, with "^{246}Cm" explicitly designated. Curium-248 was employed because of its substantially longer half-life ($t_{1/2} = 3.5 \times 10^5$ years) and accordingly lower specific radioactivity than the more plentiful ^{244}Cm isotope ($t_{1/2} = 18$ years). The U was depleted to ∼0.4% ^{235}U, and usage of "U" refers to the 99.6% ^{238}U constituent. The only naturally occurring terbium isotope, ^{159}Tb, was used.

The organic reactants were commercial products in the form of a gas or liquid used without further purification, except that the liquids were subjected to at least two freeze−evacuate−thaw cycles. The gases were admitted into the reaction zone through a pulsed valve, resulting in greater transient pressures compared with the vapors from the liquids, which were admitted through a leak valve. The vendor-specified purities were as follows: (gases) 99.99% ethene, C_2H_4; 99% propene, C_3H_6;

>99% 1-butene, C_4H_8; 99% isobutene, C_4H_8; 99.5% hexafluoropropene, C_3F_6; (liquids) 99% cyclohexene, C_6H_{10}; >99% benzene, C_6H_6; 99% 1,5-cyclooctadiene (COD), C_8H_{12}; 98% cyclooctatetraene (COT), C_8H_8; 99.9% acetonitrile, C_2H_3N.

Results and Discussion

Representative mass spectra are shown in Figures 1−4 and the principal reactivity results are presented in Tables 1−4. The tabulated product abundances, *A*, are defined as follows: $A[ML^+] = \{I[ML^+]/I[M^+]\} \times 100$, where $I[ML^+]$ and $I[M^+]$ are the mass spectral ion intensities (peak heights) for the product and unreacted metal ions, respectively. An analogous definition applies to product abundances for reactions of MO^+. These abundances correspond to the approximate percentage of parent ions that reacted only in cases of minor net reactivity, i.e., $\sum\{A[ML^+]\} < 10$; in some cases, almost all of the ablated M^+ reacted and the *A* values cannot be regarded reasonably as a percent of reacted parent ion.

In those instances where all of the significant reaction products could be confidently assigned and their summed intensities obtained, the aggregate absolute relative reaction cross sections for all reaction channels, σ_{rel}, could be estimated, because the reaction conditions (pressure and path length) were identical for coablated M^+: $\sigma_{rel}[M^+] \equiv -\log\{I[M^+]/[I[M^+] + \sum(I[ML^+])]\}$, where $I[M^+]$ represents the quantity of unreacted M^+ and $\sum(I[ML^+])$ the total quantity of all significant product ions. In general, it was impractical to obtain reliable aggregate σ_{rel} values for reactions where cracking was significant; obstacles included uncertain compositional assignments of complex product ions, minuscule amounts of ablated/unreacted U^+, and isobaric interferences, such as of CmO^+ with $UC_2H_2^+$. For some reactant substrates, such as propene, dehydrogenation was the sufficiently dominant reaction channel that $\sigma_{rel}[M^+] \approx -\log\{I[M^+]/(I[M^+] + I[MC_nH_{m-2}^+])\}$ could be reliably determined, and where such interpretation of the results is reasonable, σ_{rel} values are provided. The inability to obtain comprehensive reactivity information is intrinsic to the LAPRD technique where several ions may simultaneously react with a complex substrate to produce several reaction products. However, dehydrogenation efficiencies generally can be reliably extracted to provide comparative reaction efficiencies for that representative channel.

Vacuum Ablation of Cm_7O_{12}. Prior to carrying out the ion−molecule reactions, ablation of the target was examined under vacuum; a positive ion mass spectrum is shown in Figure 1. Ablation of AnO_2 has been shown to result in AnO^+ abundances that reflect the An−O dissociation energies, $D°[AnO]$.[25,26] Thus, Am^+ is dominant and only a minuscule amount of AmO^+ ($D°[AmO] \approx 550$ kJ mol^{-1}) is ablated from AmO_2(s), whereas copious NpO^+ ($D°[NpO] = 740$ kJ mol^{-1}) is ablated from NpO_2(s). The correlation between $D°[LnO]$ and $D°[LnO^+]$ has been discussed by Chandrasekharaiah and Gingerich[27] and suggests that IE(Ln) ≈ IE(LnO) for most Ln and that ionization of most LnO proceeds by removal of an essentially nonbonding electron localized at the metal center. Previous results for ablated AnO^+ abundances[25] indicate that a corresponding correlation exists between $D[AnO]$ and $D[AnO^+]$.

From Figure 1, it is evident that $I[Tb^+] \approx I[TbO^+]$, $I[U^+] < I[UO^+]$ and $I[Cm^+] > I[CmO^+]$. Because $D°[TbO] \approx D°[TbO^+] < D°[CmO]$, the smaller relative yield of CmO^+ compared with TbO^+ suggests that $D°[CmO^+] < D°[CmO]$ or, equivalently, that IE[CmO] > IE[Cm] and that the ionization of CmO occurs by removal of an electron from a bonding molecular orbital. The ablation of substantial UO_2^+ exhibits the stability of the U^V oxidation state, and the absence of TbO_2^+ and CmO_2^+ reflects the difficulty in oxidizing Tb and Cm beyond the trivalent state. This illustrates the trend toward lanthanide-like redox behavior beyond Pu in the actinide series. The relatively small ablation yield of U^+ compared with Cm^+ and Tb^+ reflects the oxophilicity of U and results in relatively small absolute yields of products for U^+ reactions (e.g., see the $MC_4H_6^+$ peak intensities in Figure 2).

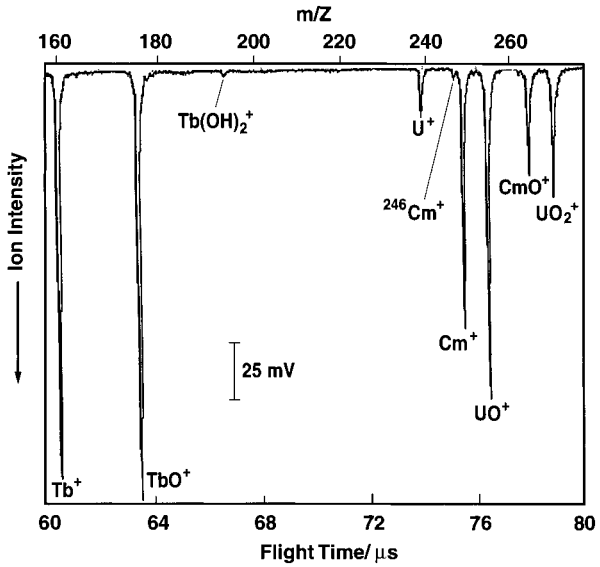

Figure 1. Mass spectrum from laser ablation of the Cm−U−Tb target in a vacuum ($t_d = 30$ μs).

Reactions with Small Alkenes. Results for the principal propene and butene reactions are presented in Table 1 and a representative mass spectrum for reactions with 1-butene is shown in Figure 2. The results for the small alkenes (C_1−C_4) are discussed separately from those for the heavier alkenes given the different injection methods used. Injection of the light alkenes through the pulsed valve, rather than leak valve, resulted in substantially greater transient pressures in the reaction zone, and direct comparisons between apparent absolute reactivities under such diverse conditions are less reliable. Specifically, it is certain that the pulsed-valve experiments resulted in a significantly greater average number of ion−molecule collisions; these collisions offer greater opportunity for reaction and for collisional cooling of ablated and complex product ions.

In addition to the results presented in Table 1, reactions were also carried out with ethene. Both Cm^+ and Tb^+ were essentially unreactive with C_2H_4; only a very small ($A \lesssim 1$) peak possibly attributable to $TbC_2H_2^+$ was noted. The reactivity of U^+ with C_2H_4 could not be assessed because $UC_2H_2^+$ is isobaric with CmO^+. No ethene adducts were detected to $A \lesssim 1$ for the M^+ and MO^+.

The comparative dehydrogenation efficiencies are emphasized in assessing the results, although reaction pathways involving C−C cleavage were significant in some cases. The alkene cracking efficiencies generally paralleled those for dehydrogenation, and it is reasonable to postulate that C−H bond activation is generally the rate-limiting step for both types of process,[28] although cracking mechanistics were not probed directly in the present LAPRD studies. In the case of propene, a particularly notable result was the distinctive formation of a significant amount of MC_2^+. A feasible mechanism for production of C_2 from propene would be dehydrogenation to propyne, followed by a single-H transfer from the α-C to the γ-C, and ultimately CH_4 elimination. This process is endothermic by ~800 kJ mol^{-1},[29] but it is possible that some M^+−C_2 bond

TABLE 1: Results for Reactions with Propene, 1-Butene, and Isobutene[a,b]

Propene[c]

		A		
	I	C_2	C_3H_4	C_3H_6
Cm^+	122	7	10	<1
U^+	1.8	*d*	500	<60
Tb^+	94	3	55	0.7
CmO^+	77			2.1
UO^+	141			0.7
TbO^+	140			1.4

1-Butene[e]

		A	
	I	C_4H_6	C_4H_8
Cm^+	102	6.3	
U^+	2.4	130	
Tb^+	94	78	
CmO^+	130	0.2	1.1
UO^+	130	0.4	<0.4
TbO^+	139	<0.1	1.4

Isobutene[c,f]

		A			
	I	C_4H_6	C_4H_8	C_8H_{12}	C_8H_{14}
Cm^+	39	130		10	14
U^+	1.8	360		39	23
Tb^+ [g]	21	230		42	84
CmO^+	82	(0.4)	6		
UO^+	88	<2	13		
TbO^+	42	(2)	24		

[a] The following definitions apply to all of the tabulated results. *I* = intensity (peak height) of the specified reactant ion in millivolts (corresponds to intensity scales in the figures). *A* = abundance of the ML^+ or MOL^+ for the specified L (of indeterminate structure): $A[ML^+] / \{I[ML^+]/I[M^+]\} \times 100$; $A[MOL^+]/\{I[MOL^+]/I[MO^+]\} \times 100$. The reported abundances are uncertain to the greater of 10% or one digit in the last recorded significant figure. Where appropriate, estimated abundance limits are provided for undetected products. Abundances presented in parentheses represent measurements close to the detection limit. The following approximate aggregate relative reaction cross sections, $\sigma_{rel}[M^+]$, could be derived: (propene) 0.8 for U^+, 0.2 for Tb^+, and 0.04 for Cm^+; (1-butene) 0.4 for U^+, 0.3 for Tb^+, and 0.03 for Cm^+. [b] Pulsed valve. [c] $t_d = 60$ μs. [d] UC_2^+ is isobaric with $^{246}CmO^+$. [e] $t_d = 50$ μs; $A[TbC_2H_2^+] = 12$; mass spectrum shown in Figure 2. [f] Dehydrogention was dominant but significant cracking was evident (e.g., minor $MC_3H_4^+$). [g] $A[TbC_2H_2^+] = 210$ ($A[CmC_2H_2^+] < 10$; $UC_2H_2^+$ is isobaric with CmO^+).

energies are of this magnitude,[27] and hyperthermal (and/or electronically excited) M^+ could be important in thermodynamically enabling this process. For the more prevalent propene dehydrogenation process, formation of propadiene rather than propyne is slightly less endothermic[27] and is mechanistically more feasible, presuming relatively facile insertion of M^+ into the terminal allylic C−H bond followed by β−H abstraction. The $A[MC_3H_4^+]$ values in Table 1 indicate an order of propene dehydrogenation efficiency of $U^+ > Tb^+ > Cm^+$. Because dehydrogenation was the dominant reaction pathway, the following approximate σ_{rel} can be derived readily from the data in Table 1, 0.8 for U^+, 0.2 for Tb^+, and 0.04 for Cm^+. The three MO^+ were unreactive, each producing roughly comparable yields of the MO^+−propene adduct.

As with propene, the primary reaction channel for the M^+ with 1-butene and isobutene was dehydrogenation, and again, the order of reactivity was $U^+ > Tb^+ > Cm^+$. The σ_{rel} values for dehydrogenation of 1-butene were 0.4 for U^+, 0.3 for Tb^+, and 0.03 for Cm^+. In contrast to propene, a minor degree of

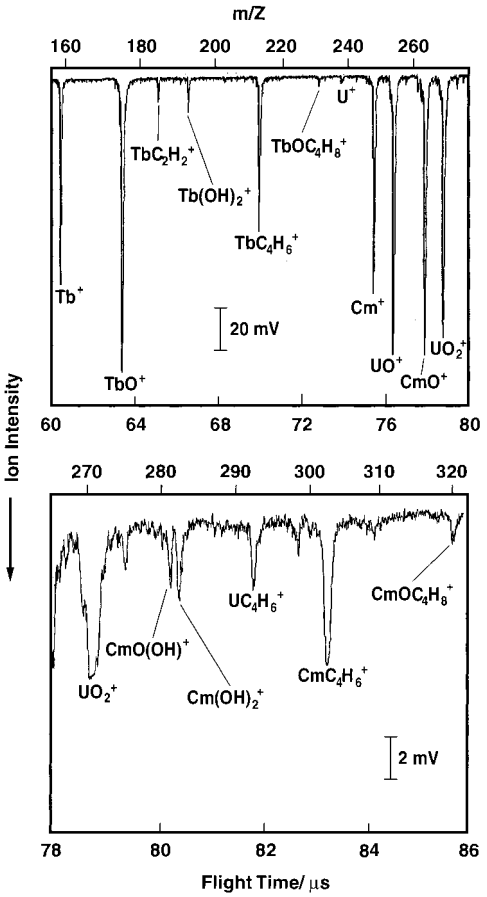

Figure 2. Mass spectrum from laser ablation of the Cm−U−Tb target into 1-butene ($t_d = 50$ μs).

dehydrogenation was effected by the MO^+ with the butene substrates, suggesting enhanced MO^+−C_4H_8 coupling to form a multicentered activation complex. With isobutene, cracking by the M^+, particularly C_2H_6 elimination ($MC_2H_2^+$ product), and notably CH_4 elimination ($MC_3H_4^+$ product) were significant pathways. Because of isobaric interferences (e.g., $UC_2H_2^+$ is isobaric with CmO^+) and the significant degree of cracking, reliable aggregate σ_{rel} values could not be derived for these reactions, but the order of dehydrogenation efficiencies was consistent with that for the 1-butene, $U^+ > Tb^+ > Cm^+$.

Speculating on possible isobutene cracking reaction mechanisms, CH_4 loss, for example, might reflect a relatively facile transfer of the activated allylic H atom to the intact CH_3 group; in contrast, formation of propadiene from 1-butene would require an additional intramolecular H migration from the β-C to the terminal γ-C. Isobutene was also distinguished by the formation of products resulting from interaction of the M^+ with two reactant molecules; $MC_8H_{12}^+$ corresponds to net double dehydrogenation of two C_4H_8 molecules and $MC_8H_{14}^+$ to single dehydrogenation of a C_4H_8 and complexation of a second C_4H_8. Because $MC_4H_4^+$ was not a significant product, it can be assumed that the $MC_8H_{12}^+$ resulted primarily from dehydrogenation of a second C_4H_8 by a predecessor $MC_4H_6^+$. This would suggest that the metal center of the $MC_4H_6^+$ complexes remained reactive and that the M^+−C_4H_6 bonding is best represented as an interaction of the metal center with the C=C π system, as a σ-bonded metallocyclic complex would presumably render the metal valence electrons inert toward subsequent C−H activation. The comparative abundances of the $MC_8H_{12}^+$ and $MC_8H_{14}^+$ products suggest that U^+−C_4H_6 is more efficient at dehydrogenating a second C_4H_8 than are either Cm^+−C_4H_6

TABLE 2: Results for Reactions with Cyclohexene and Benzene[a]

Cyclohexene[b]

	I	*A*[C_6H_6]
Cm^+	59	5
U^+	1.5	7
Tb^+	23	13
CmO^+	6.2	2
UO^+	5.6	2
TbO^+	10	<3

Benzene[c]

		A	
	I	C_6H_4	C_6H_6
Cm^+	614	0.03	0.05
U^+	4.7	2	<0.5
Tb^+	340	(0.07)	0.14

[a] See footnote a of Table 1. [b] t_d = 55 μs. A mass spectrum corresponding to t_d = 35 μs is shown in Figure 3; the longer t_d allowed detection of the $MOC_6H_6^+$ products. [c] t_d = 35 μs. No adducts or reaction products were detected for the MO^+. The following approximate relative benzene dehydrogenation cross sections, $\sigma_{rel}[M^+]$, could be derived: 1×10^{-2} for U^+, 3×10^{-4} for Tb^+, and 1×10^{-4} for Cm^+.

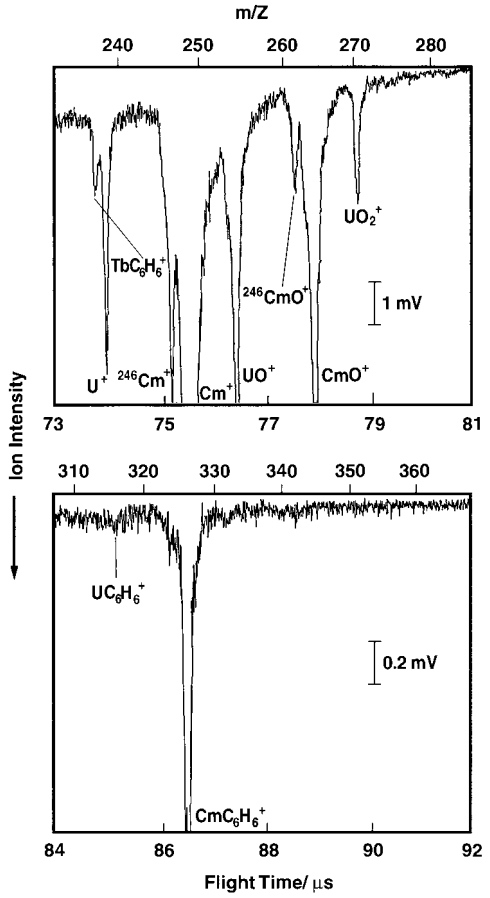

Figure 3. Mass spectrum from laser ablation of the Cm−U−Tb target into cyclohexene (t_d = 35 μs). The off-scale peak intensities (in millivolts) are as follows: *I*[Tb^+] = 292; *I*[TbO^+] = 63; *I*[Cm^+] = 340; *I*[UO^+] = 34; *I*[CmO^+] = 38.

or Tb^+−C_4H_6. This finding may constitute a manifestation of the greater chemical activity of the uranium 5f electrons.

Reactions with C_6 and C_8 Cycloalkenes. Results for reactions with cycloalkenes are compiled in Tables 2 and 3. Representative LAPRD mass spectra for reactions with cyclohexene and COD are shown in Figures 3 and 4, respectively. The primary reaction pathway with C_6H_{10} was double dehydrogenation to produce $MC_6H_6^+$, presumably a M^+−benzene complex, and $MOC_6H_6^+$, presumably a O=M^+−benzene com-

TABLE 3: Results for Reactions with 1,5-Cyclooctadiene (COD) and Cyclooctatetraene (COT)[a]

COD[b]

		A			
	I	C_2H_2	C_6H_6	C_8H_6	C_8H_8
Cm^+	128	1.4	1.8	1.6	7
U^+	1.1	*c*	<10	<10	(16)
Tb^+	30	5	6	2.5	22

COT[d]

		A	
	I	C_8H_6	C_8H_8
Cm^+	7.4	34	24
U^+	(0.4	<3	6)
Tb^+	2.9	10	16
CmO^+	4.9	<3	<3
UO^+	2.8	<2	3
TbO^+	3.8	<3	<3

[a] See footnote a of Table 1. [b] t_d = 45 μs. Also, *A*[$TbOC_8H_{10}^+$] = 2.9; *A*[$CmOC_8H_{10}^+$] = 1.9; *A*[$UOC_8H_{10}^+$] < 2; *A*[$UO_2C_8H_{12}^+$] = 4. Mass spectrum shown in Figure 4. The following approximate aggregate relative reaction cross sections, $\sigma_{rel}[M^+]$, could be derived for COD: 0.13 for Tb^+ and 0.05 for Cm^+. [c] $UC_2H_2^+$ is isobaric with CmO^+. [d] t_d = 55 μs. Also, significant amounts of various cracking products, e.g., *A*[$CmC_6H_6^+$] = 16, were observed.

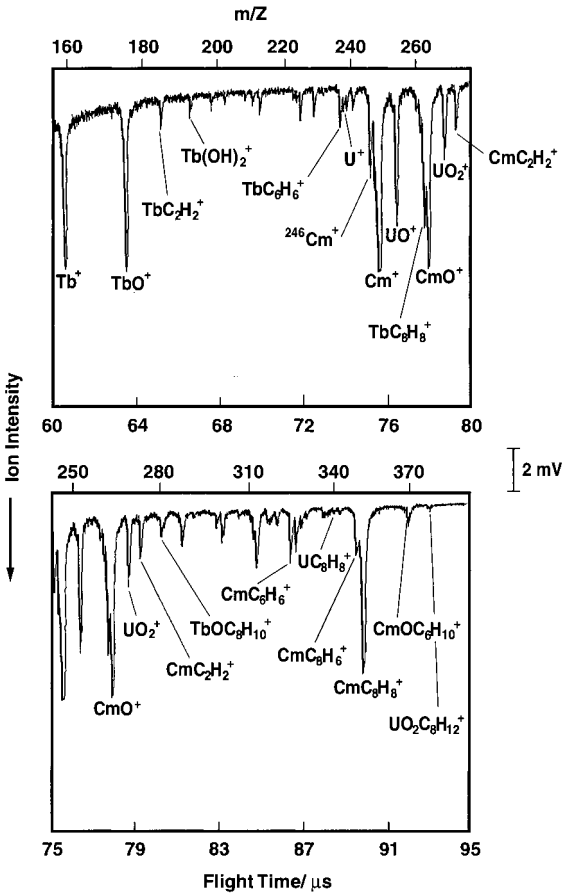

Figure 4. Mass spectrum from laser ablation of the Cm−U−Tb target into 1,5-cyclooctadiene (t_d = 45 μs). The Tb^+, TbO^+, Cm^+, and CmO^+ peaks are off-scale at this detection sensitivity; intensities are given in Table 3.

plex. As noted above, the substantially smaller abundances of the product ions compared with the corresponding propene and butene reactions (Table 1) are considered to reflect the lower pressures achieved with these less volatile reactants. In contrast to the substantial variations in reactivities with propene and the butenes, the dehydrogenation efficiencies of Cm^+, U^+, and Tb^+ toward C_6H_{12} were roughly comparable (i.e., within a factor of 3). This apparent reduction in the role of electronic excitation to achieve a d^1s^1 configuration may be attributable to a deeper energy well for the initial $M^+-C_6H_{10}$ adduct on the dehydrogenation reaction coordinate, which would facilitate "curve-crossing" to produce the $C-M^+-H$ intermediate.[4] Similarly, the apparent greater relative efficiency of the MO^+ at dehydrogenating C_6H_{10}, compared with the small alkenes, may reflect stronger bonding in the $MO^+-C_6H_{10}$ multicentered activation complexes. Dehydrogenation of cyclohexene to benzene is also facilitated by an endothermicity of only 88 kJ mol^{-1}.[29,30]

As expected from the greater energy required to dehydrogenate benzene to benzyne (360 kJ mol^{-1}), the dehydrogenation efficiencies with benzene were relatively small, particularly for Cm^+ and Tb^+ (both produced small amounts of $MC_6H_6^+$ adducts). As seen from the results in Table 2, U^+ was relatively effective at dehydrogenating benzene; this may also imply unique participation of the 5f electrons in the reaction mechanism and in the ultimate $U^+-C_6H_4$ (presumably benzyne) complex. Because dehydrogenation was the primary (minor) reaction pathway, the following σ_{rel} values for dehydrogenation of benzene can be derived: 1×10^{-2} for U^+, 3×10^{-4} for Tb^+, and 1×10^{-4} for Cm^+. Given the energetic requirement for benzene dehydrogenation, it is can be presumed that the $U^+-C_6H_4$ complex must exhibit unusually robust bonding. A feasible structure is a σ-bonded metallocyclic moiety at the dehydrogenated C═C site, with supplementary bonding of the U^+ to the benzyl ring, perhaps involving interaction of the π system with the 5f electrons and orbitals at the U metal center.

The mass spectrum shown in Figure 4 for reaction with COD exhibits the greater diversity of reaction channels for this substrate. In addition to the primary dehydrogenation channels, cracking to C_2H_2 (presumably acetylene) and C_6H_6 (presumably benzene) were also significant. Double dehydrogenation to $MC_8H_8^+$, presumably a M^+-COT complex, was dominant, and the other reactions proceeded with roughly parallel relative efficiencies (although $I[U^+]$ was too small to obtain precise comparisons). As with cyclohexene, the dehydrogention efficiencies of Cm^+, U^+, and Tb^+ were approximately comparable, with Tb^+ somewhat more reactive than Cm^+. As indicated in Table 3, the results for U^+ are incomplete but aggregate σ_{rel} values of 0.13 and 0.05 are obtained for Tb^+ and Cm^+, respectively.

With COT, $I[U^+]$ was very small, and only an approximate adduct abundance is given in Table 3. A notable result for uranium was the distinctive formation of the UO^+-COT adduct; this again may reflect bonding involving 5f electrons in a O═ $U^+-C_8H_8$ complex. Assigning a nominal charge of -2 to the COT ligand, this species would represent a M^V organometallic complex, which is implausible for Cm or Tb. In contrast to results for the reactions of M^+ with the other substrates, it appears that Cm^+ may be moderately more effective at dehydrogenating COT than is Tb^+. However, this effect was small compared with the substantial reactivity discrepancies for the smaller alkenes and it should be noted that significant amounts of cracking products were produced (but not quantitatively assessed) and their contribution to the overall reactivities may have distorted the relative reactivity assessment based upon the abundances of the dehydrogenation products. The main

TABLE 4: Results for Reactions with Acetonitrile and Hexafluoropropene[a]

Acetonitrile[b]

		A	
	I	CHCN	CH_3CN
Cm^+	1260	0.07	0.27
U^+	3.1	21	6
Tb^+	470	0.6	0.4
CmO^+	88	<0.3	1.8
UO^+	47	0.5	8
TbO^+	165	<0.2	2.1

Hexafluoropropene[c]

		A			
	I	F	F_2	F_3	F_4
Cm^+	118	5	6	<0.1	<0.1
U^+	19	40	25	15	3.4
Tb^+	82	10	13	<0.2	<0.2
CmO^+	45	<0.3	<0.3	<0.1	<0.1
UO^+	153	2	0.9	0.12	<0.1
TbO^+	62	<1	<0.2	<0.2	<0.2

[a] See footnote a of Table 1. [b] Leak valve; $t_d = 50$ μs. Also, $A[UO_2CH_3CN^+] = 8$. The following approximate aggregate relative reaction cross sections for acetonitrile, $\sigma_{rel}[M^+]$, could be derived: 8×10^{-2} for U^+, 3×10^{-3} for Tb^+, and 3×10^{-4} for Cm^+. [c] Pulsed valve; $t_d = 60$ μs.

significance of the COT results was the substantial yields of the adducts, indicating strong M^+-COT bonding. All of the $I[M^+]$ values were small, and $I[U^+]$ was too small to obtain quantitative results; depletion of the M^+ is attributed to the high degree of adduct formation and abundant reaction products, including the dehydrogenation product specified in Table 3 and the cracking products such as $MC_6H_6^+$ (see Figure 4).

Reactions with Acetonitrile. The results obtained with acetonitrile as the reactant are recorded in Table 4. All three M^+ formed adducts with acetonitrile, presumably involving coordination to the C≡N**:** moiety and particularly its lone pair of electrons. All three M^+ also dehydrogenated acetonitrile, presumably via "side-on" (rather than the usual end-on) coordination of the M^+ to the C≡N**:** functionality.[32] The MC_2HN^+ dehydrogenation products are surmised to be the distinctive M^+═(CH)−C≡N carbene complexes proposed for the corresponding reactions of Sc^+ and Y^+ with acetonitrile.[31] Dehydrogenation was the primary reaction pathway for all three M^+ and the following σ_{rel} were derived from the results: 8×10^{-2} for U^+, 3×10^{-3} for Tb^+, and 3×10^{-4} for Cm^+. The typical discrepancies between dehydrogenation efficiencies, $U^+ > Tb^+ > Cm^+$, was clearly evident with this substrate. Each of the MO^+ ions complexed to CH_3CN, with the abundance being the greatest for UO^+. Furthermore, among the oxoligated ions, only UO^+ effected detectable dehydrogenation, again suggesting distinctive chemical activity of the 5f electrons at the metal center of UO^+.

Interpretation of Dehydrogenation Reactions. On the basis of the energies for the $f^{n-1}s^1$ to $f^{n-2}d^1s^1$ promotions of U^+, Cm^+, and Tb^+ (vide supra), it would be anticipated that U^+ should be more effective at dehydrogenating alkenes and nitriles than the two other M^+, a prediction corroborated by our results. The $f^{n-1}s^1$ to $f^{n-2}d^1s^1$ promotion energy for Cm^+ is only slightly greater than that of Tb^+ ($\Delta[PE] = 9$ kJ mol^{-1}), and a greater chemical activity of the actinide's 6d vs the lanthanide's 5d electrons could diminish the effect of this discrepancy. Accordingly, it was anticipated that the dehydrogenation efficiencies of Cm^+ and Tb^+ would be virtually identical within the discrimination capabilities of the LAPRD technique, and the

significantly greater dehydrogenation efficiency of Tb^+ vs Cm^+, particularly with the propene, butene, and acetonitrile substrates, was unexpected in the context of the simple $f^{n-1}s^1 \rightarrow f^{n-2}d^1s^1$ mechanistic model. The greater reactivity of Tb^+ can be rationalized by more closely considering the requisite electronic transitions for achieving the activated intermediate. Specifically, the transition from the odd ^7H $4f^96s^1$ ground state of Tb^+ to the even ^9G $4f^85d^16s^1$ configuration is parity-allowed, whereas the odd ^8S $5f^77s^2$ to odd ^{10}D $5f^76d^17s^1$ transition for Cm^+ is parity forbidden. It is reasonable that the effects of the discrepancy in transition probabilities should be most pronounced with those small alkene substrates where the energy well of the initial adduct intermediate is relatively shallow and the weaker M^+-alkene interaction does not relax effectively the transition selection rules. Both the Tb^+ ^9G and Cm^+ ^{10}D prepared "divalent" configurations are high-spin states with spin-unpaired d and s valence electrons; however, it is plausible that different effects due to spin nonconservation between lanthanides and actinides with regard to the insertion process may alter their relative reaction efficiencies.

Reactions with Hexafluoropropene. The product abundance distributions for reactions with hexafluoropropene are included in Table 4. The primary reaction pathway for reactions of Ln^+, An^+, LnO^+, and AnO^+ is F abstraction via a noninsertion mechanism,[21-24] and the product compositions and abundances reflect the elementary oxidation−reduction behavior of the metal. With regard to fluorine abstraction, Cm^+ and Tb^+ behaved similarly, producing the divalent MF^+ and trivalent MF_2^+ species. In contrast, U^+ abstracted up to four F atoms, producing UF^+, UF_2^+, UF_3^+, and pentavalent UF_4^+. As has been discussed elsewhere,[24] the thermochemical propensity for formation of MF_n^+ by F abstraction from fluorocarbons can be considered in the context of ionic, covalent, or intermediate bonding models, with the degree of covalency increasing with increasing oxidation state of the metal. The behavior observed here is consistent with the greater $M^{3+} \rightarrow M^{4+}$ ionization energies for Cm^{3+} (IE = 3550 kJ mol^{-1} [33]) and Tb^{3+} (3840 kJ mol^{-1} [17]) as compared to that of U^{3+} (3140 kJ mol^{-1}). The bonding is likely to be substantially covalent in MF_3^+ and the promotion energies to provide a non-f valence electron are also consistent with the distinctive formation of UF_3^+ (and UF_4^+); the PE[$M^{3+}\{f^n\} \rightarrow M^{3+}\{f^{n-1}d^1\}$] values have been estimated by Brewer[34] as ~360, ~820, and ~720 kJ mol^{-1} for U^{3+}, Cm^{3+}, and Tb^{3+}, respectively. In accord with the oxidation limit of Cm and Tb being at the trivalent state, among the MO^+, only UO^+ abstracted fluorine, to produce UOF^+, UOF_2^+, and even the hexavalent species, UOF_3^+. Gas-phase fluorination reactions, such as those achieved by F abstraction from gaseous C_nF_m, reflect the essential oxidation−reduction chemistry exhibited in the condensed phase. Thus, whereas the hexavalent state is prevalent for uranium, the trivalent state dominates for curium in the region of the actinide series where lanthanide-like behavior is manifested.[35]

Summary and Conclusions

The first systematic gas-phase studies exploring the chemistry of curium were performed employing elementary reaction substrates that had been studied previously with lighter actinides. Uranium and terbium were studied concurrently with curium to permit assessing directly relative reactivities. Vacuum ablation of curium oxide produced a smaller yield of CmO^+ than anticipated based upon the known $D°$[CmO], and this result is interpreted as IE[CmO] > IE[Cm]. Reactions with alkenes focused on dehydrogenation efficiencies, although cracking efficiencies were generally in correspondence. The key conclusion was that Cm^+ is substantially less effective than U^+ and somewhat less effective than Tb^+ at alkene dehydrogenation. The lower reactivity of Cm^+ vs U^+ is consistent with C−H activation via a $C-An^+-H$ insertion intermediate that requires two non-5f electrons at the metal center for covalent bonding. The reduced reactivity of ground-state Cm^+ indicates that its spin-paired $7s^2$ electrons are chemically inert, like the $6s^2$ electrons of Lu^+, the $3s^2$ electrons of Mg^o, and presumably the $7s^2$ electrons of ground-state U^+, and that decoupling by excitation to a $6d^17s^1$ configuration is requisite for effective insertion. The reduced reactivity of Cm^+ compared with Tb^+ was somewhat greater than anticipated based upon their similar promotion energies; it should be emphasized that this effect was secondary to the primary finding of significantly reduced reactivity of Cm^+ compared with U^+, which demonstrated the necessity for excitation from the s^2 ground-state configuration of Cm^+. Assuming that the Cm^+ electronic energy level assignments are correct, its unanticipated degree of diminished reactivity compared with Tb^+ might be attributed to the parity-forbidden nature of the essential odd $5f^77s^2 \rightarrow$ odd $5f^76d^17s^1$ transition. Other factors might be involved in this diminished reactivity, such as indistinct spin-conservation effects, contraction of the chemically relevant M^+ valence orbitals, variable M^+ polarizabilities, and indeterminate relativistic effects. It is hoped that these experimental results will motivate further elucidation of relevant effects employing theoretical models. The MO^+ were substantially less reactive than the naked M^+ but comparably reactive to one another, consistent with a mechanism involving a multicentered activation complex, as suggested previously.[14] Certain peculiarities of UO^+, such as its distinctive formation of an adduct with COT, were consistent with previous indications of chemically active 5f electrons at the uranium metal center. Evidence was not obtained for involvement of curium's 5f electrons in bonding.

All three M^+ dehydrogenated acetonitrile, with efficiencies in accord with the insertion requirements inferred for the alkenes. The dehydrogenation products are presumed to be novel carbenes, including $Cm^+{=}CD-C{\equiv}N$:. Among the oxide ions, only UO^+ effectively dehydrogenated acetonitrile, exhibiting the unique chemistry of uranium, which is presumably related to more chemically active 5f-electrons. Attesting to the strongly coordinating nature of the C≡N: functionality, all of the M^+ and MO^+ species formed adducts with acetonitrile.

The reaction product compositions and abundance distributions for reactions of M^+ and MO^+ with hexafluoropropene reflected the essential oxidation behaviors of the elements studied. Oxidation of Cm and Tb terminated at the trivalent state as MF_2^+ and MO^+, despite the fact that both are known to form tetravalent compounds under strongly oxidizing conditions. In contrast, uranium was oxidized to pentavalent UF_4^+ and hexavalent UOF_3^+. As has been discussed before,[23] such discrepancies in the propensities of An^+ and AnO^+ to abstract F atoms from simple fluorocarbons may be applicable to separating isobaric elements for mass analysis or possibly even for separations processes. There was no indication of mechanistic constraints, and fluoride abstraction is presumed to have proceeded by a noninsertion ("harpoon") process.

Acknowledgment. This work was sponsored by the Division of Chemical Sciences, Office of Basic Energy Sciences, U. S. Department of Energy, under Contract DE-AC0596OR22464 at the Oak Ridge National Laboratory with Lockheed Martin Energy Research Corp. The ^{248}Cm used in this study was supplied by the Division of Chemical Sciences, Office of Energy

Research, U. S. Department of Energy, through the transplutonium element production facilities located at the Oak Ridge National Laboratory.

References and Notes

(1) (a) Eller, K.; Schwarz, H. *Chem. Rev.* **1991**, *91*, 1121−1177. (b) Schroder, D.; Hrusak, J.; Tornieporth-Oetting, I. C.; Klapotke, T. M.; Schwarz, H. *Angew. Chem., Int. Ed. Engl.* **1994**, *33*, 212−214.

(2) Freiser, B. S., Ed. *Organometallic Ion Chemistry*; Kluwer: Dordrect, 1996.

(3) (a) Huang, Y.; Wise, M. B.; Jacobson, D. B.; Freiser, B. S. *Organometallics* **1987**, *6*, 346−354. (b) Beauchamp, J. L.; Schilling, J. B.; *J. Am. Chem. Soc.* **1988**, *110*, 15−24. (c) Sunderlin, L. S.; Armentrout, P. B. *J. Am. Chem. Soc.* **1989**, *111*, 3845−3855. (d) Heinemann, C.; Schroder, D.; Schwarz, H. *Chem. Ber.* **1994**, *127*, 1907−1810. (e) Yin, W. W.; Marshall, A. G.; Marcalo, J.; Pires de Matos, A. *J. Am. Chem. Soc.* **1994**.

(4) Cornehl, H. H.; Heinemann, C.; Schroder, D.; Schwarz, H. *Organometallics* **1995**, *14*, 992−999.

(5) Gibson, J. K. *J. Phys. Chem.* **1996**, *100*, 15688−15694.

(6) Cornehl, H. H.; Wesendrup, R.; Harvey, J. N.; Schwarz, H. *J. Chem. Soc., Perkin Trans. 2* **1997**, 2283−2291.

(7) (a) Armentrout, P.; Hodges, R.; Beauchamp, J. L. *J. Am. Chem. Soc.* **1977**, *99*, 3162−3163. (b) Armentrout, P. B.; Hodges, R. V.; Beauchamp, J. L. *J. Chem. Phys.* **1977**, *66*, 4683−4688.

(8) Heinemann, H.; Cornehl, H. H.; Schwarz, H. *J. Organomet. Chem.* **1995**, *501*, 201−209.

(9) Marcalo, J.; Leal, J. P.; Pires de Matos, A. *Int. J. Mass Spectrom. Ion Processes* **1996**, *157/158*, 265−274.

(10) Marcalo, J.; Pires de Matos, A. *Organometallics* **1997**, *16*, 3845−3850.

(11) Gibson, J. K. *Organometallics* **1997**, *16*, 4214−4222.

(12) Marcalo, J.; Leal, J. P.; Pires de Matos, A. *Organometallics* **1997**, *16*, 4518−4588.

(13) Cornehl, H. H.; Wesendrup, R.; Diefenbach, M.; Schwarz, H. *Chem.−Eur. J.* **1997**, *3*, 1083−1090.

(14) Gibson, J. K. *J. Am. Chem. Soc.* **1998**, *120*, 2633−2640.

(15) Gibson, J. K. *Organometallics* **1998**, *17*, 2583−2589.

(16) Fred, M. S.; Blaise, J. In *The Chemistry of the Actinide Elements*, 2nd ed.; Katz, J. J., Seaborg, G. T., Morss, L. R., Eds.; Chapman and Hall: London, 1986; pp 1196−1277.

(17) Martin, W. C.; Zalubas, R.; Hagan, L. *Atomic Energy Levels − The Rare Earth Elements*; National Bureau of Standards: Washington, DC, 1978; pp 250−254.

(18) Eller, K.; Zummack, W.; Schwarz, H. *J. Am. Chem. Soc.* **1990**, *112*, 621−627.

(19) Eller, K. *Coord. Chem. Rev.* **1993**, *126*, 93−147.

(20) Gibson, J. K. *Inorg. Chem.*, in press.

(21) Heinemann, C.; Goldberg, N.; Tornieporth-Oetting, I. C.; Klapotke, T. M.; Schwarz, H. *Angew. Chem., Int. Ed. Engl.* **1995**, *34*, 213-217.

(22) Cornehl, H. H.; Hornung, G.; Schwarz, H. *J. Am. Chem. Soc.* **1996**, *118*, 9960−9965.

(23) Gibson, J. K. *J. Fluorine Chem.* **1996**, *78*, 65−74.

(24) Gibson, J. K. *Radiochim. Acta*, submitted.

(25) Gibson, J. K. *Radiochim. Acta* **1998**, *81*, 83−92.

(26) Haire, R. G. *J. Alloys Compounds* **1994**, *213/214*, 185−190.

(27) Chandrasekhariah, M. S.; Gingerich, K. A. In *Handbook on the Physics and Chemistry of Rare Earths*; Gschneidner, K. A., Jr., Eyring, L., Eds.; North-Holland: Amsterdam, 1989; Vol. 12, pp 409−431.

(28) van Koppen, P. A. M.; Bowers, M. T.; Haynes, C. L.; Armentrout, P. B. *J. Am. Chem. Soc.* **1998**, *120*, 5704−5712.

(29) Lias, S. G.; Bartmess, J. E.; Liebman, J. F.; Holmes, J. L.; Levin, R. D.; Mallard, W. G. *Gas-Phase Ion and Neutral Thermochemistry*; American Chemical Society: Washington, DC, 1988.

(30) Mallard, W. G., Linstrom, P. J., Eds. *NIST Chemistry WebBook*; NIST Standard Reference Database 69; National Institute of Standards and Technology: Gaithersburg, MD, 1998 (http://webbook.nist.gov).

(31) Wilson, K. L.; Cooper, B. T.; Buckner, S. W. *Rapid Commun. Mass Spectrom.* **1993**, *7*, 844−847.

(32) Lebrilla, C. B.; Drewello, T.; Schwarz, H. *Organometallics* **1987**, *6*, 2450−2451.

(33) Morss, L. R. In *The Chemistry of the Actinide Elements*, 2nd ed.; Katz, J. J., Seaborg, G. T., Morss, L. R., Eds.; Chapman and Hall: London, 1986; pp 1278−1360.

(34) Brewer, L. *J. Opt. Soc. Am.* **1971**, *61*, 1666−1682.

(35) Katz, J. J.; Morss, L. R.; Seaborg, G. T. In *The Chemistry of the Actinide Elements*, 2nd ed.; Katz, J. J., Seaborg, G. T., Morss, L. R., Eds.; Chapman and Hall: London, 1986; pp 1121−1195.